



	Experiment title: The FCC-HCP boundary in lead	Experiment number: HS-1420
Beamline: ID30	Date of experiment: from: 28/04/2001 to: 02/05/2001	Date of report: 13/09/2001 <i>Received at ESRF:</i>
Shifts: 12	Local contact(s): P.Bouvier	

Names and affiliations of applicants (* indicates experimentalists): Vladimir DMITRIEV* - SNBL/ESRF (Grenoble, France) Leonid DUBROVINSKY* - Institute of Earth Science, Uppsala University (Uppsala, Sweden) Vitaliy PROKOPENKO* - Institute of Earth Science, Uppsala University (Uppsala, Sweden) Alexei KUZNETSOV* - SNBL/ESRF (Grenoble, France) Hans-Peter WEBER* - SNBL/ESRF (Grenoble, France)		
--	--	--

Report:

Face-centred cubic (fcc) and hexagonal close-packed (hcp) structures co-exist in the pressure-temperature phase diagrams of more than twenty elemental crystals [1], but only for six of them (He, Fe, Co, Tl, Pb and Yb) there is direct fcc-hcp transformation. On the other hand in Fe, Tl and Yb, the bcc phase occupies a large region surrounding both, fcc and hcp phases. In those three elements one can thus deduce the fcc and hcp structures from the bcc structure via the Bain deformation and Buegers mechanisms. This is not the case for He, Co and Pb in the phase diagram of which the bcc structure is either absent (as in Co) or located far from the region of co-existence of the fcc and hcp phases (as in He and Pb). For Co and He it has led [2] to give an interpretation of the fcc-hcp transformation in terms of a re-ordering process, involving a disordered polytype structure [2,3] which implies a number of specific features for the transformation, and especially an asymmetry for some of its physical properties (as for example the latent heat on cooling and heating [4]).

The phase diagram of lead is almost unexplored [5], and the Pb(I)-Pb(II) (fcc-hcp) transformation has been detected [4,6] only at room temperature, at which it occurs between 13 and 16 GPa.

We performed angle dispersive X-ray diffraction studies of three different samples of high purity lead (Advent, 99.999%) and using two diamond anvil cells externally heated. All experiments employed NaCl and its equation of state [7] for pressure determination. Diffraction patterns were recorded with an image plate detector (MAR345) and integrated with FIT2D program [8]. The lattice parameters with standard deviations were obtained using the program CHEKCELL.

In Fig.1 we report the phase diagram of lead in the temperature range 300-800 K and pressure below 26 Gpa.

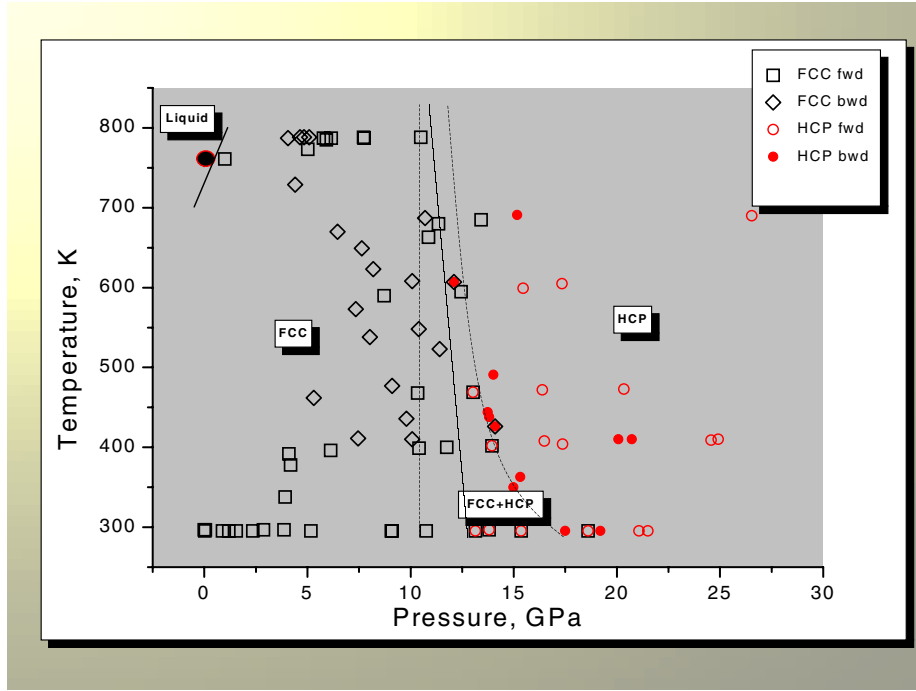


Fig. 1. Phase diagram of lead and the lines of stability of FCC and HCP phases.

The following Birch-Murnaghan EOS was fitted to the experimental data:

$$P(V, T) = \frac{3}{2} B(T) \cdot (x^{7/3} - x^{5/3}) \cdot \left(1 + \frac{3}{4} \cdot (B'(T) - 4) \cdot (x^{2/3} - 1) \right).$$

Here $x = \frac{V(T,0)}{V}$, V is the volume per atom, and $V(T,0)$ is the extrapolated volume per atom of the phase under consideration at zero pressure and at temperature equal T .

$$V(T,0) = V(T_0,0) \cdot \exp\left(\int_{T_0}^T \alpha(T) dT\right) = V(T_0,0) \cdot \exp\left(\int_{T_0}^T (\alpha_0 + \alpha_1 \cdot T + \alpha_2 \cdot T^2 + \alpha_3 \cdot T^3 + \alpha_4 \cdot T^4) dT\right) \cong$$

$$V(T_0,0) \cdot \left(1 + \alpha_0 \cdot (T - T_0) + \frac{1}{2} \alpha_1 \cdot (T - T_0)^2 + \frac{1}{3} \alpha_2 \cdot (T - T_0)^3 + \frac{1}{4} \alpha_3 \cdot (T - T_0)^4 + \frac{1}{5} \alpha_4 \cdot (T - T_0)^5 \right),$$

$$B(T) = B_0 + \beta_1 \cdot (T - T_0) + \beta_2 \cdot (T - T_0)^2, \quad \text{and} \quad B'(T) = B'_0 + \beta' \cdot (T - T_0). \quad B_0, B'_0, V(T_0,0), \alpha_0, \alpha_1, \alpha_2, \alpha_3, \alpha_4, \beta_1, \beta_2, \beta'$$

are fitting parameters. Main results are presented below in Fig.2.

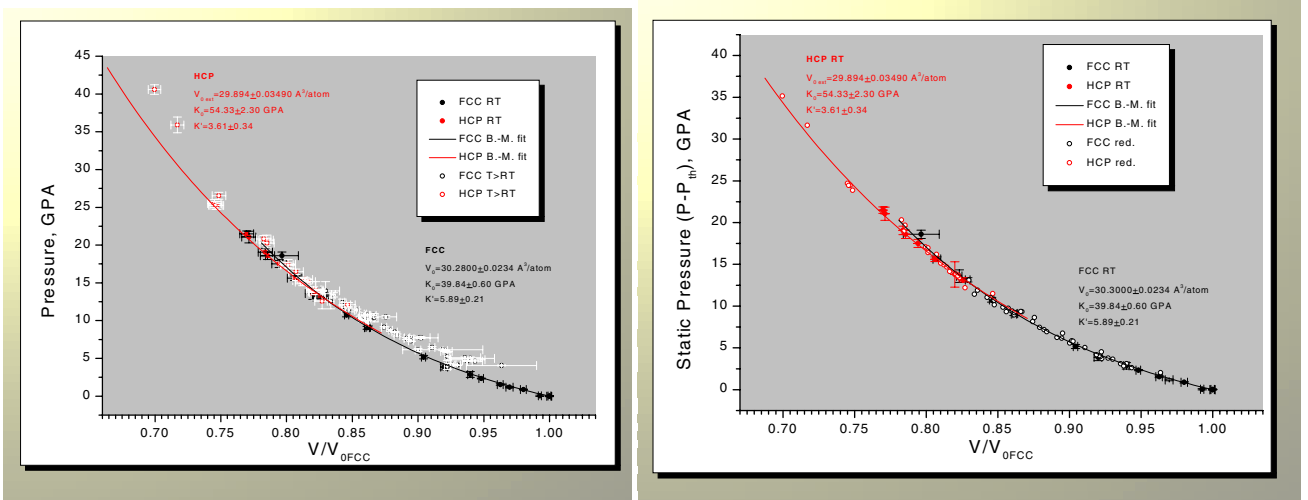


Fig. 2. a) Projection of data points of FCC and HCP phases on P - V plane; b) Static part of pressure for measured points.

Table of parameters for EOS.

Parameter	FCC phase	HCP phase
$V(296,0)$	121.2000	59.7880
B_0	39.84	54.33
β_1	$-2.92 \cdot 10^{-3}$	$-4.99 \cdot 10^{-2}$
β_2	$-4.91 \cdot 10^{-5}$	$2.16 \cdot 10^{-5}$
B_0'	5.89	3.61
β'	$1.03 \cdot 10^{-3}$	$4.65 \cdot 10^{-3}$
α_0	$8.67 \cdot 10^{-5}$	$8.43 \cdot 10^{-5}$
α_1	$1.57 \cdot 10^{-9}$	$1.24 \cdot 10^{-9}$
α_2	$2.37 \cdot 10^{-11}$	$6.39 \cdot 10^{-13}$
α_3	$2.91 \cdot 10^{-13}$	0
α_4	$3.08 \cdot 10^{-15}$	0

1. D. A. Young, *Phase Diagrams of the Elements* (U. of California Press, Berkeley, 1991.)
2. V.P. Dmitriev et al, *Phys. Rev. Letters* **62** (1989) 2495.
3. P. Tolédano et al., *Phys. Rev. B* **64** (2001).
4. R. Adams and C. Alstetter, *JMS-AIME* **242** (1968) 139.
5. A) Ref. [1], p. 108; B. Vanderborgh, C.A., Vohra, Y.K., Xia, H. and Ruoff, A.L., *Phys. Rev. B* **41** (1990) 7338-7340; B) C. Godwal, B.K., Meade, C., Jeanloz, R., Garcia, A., Liu, A.Y., Cohen. M., *Science* **248** (1990) 462.
6. A.S. Balchass and H.G. Drickamer, *Rev. Sci. Instrum.* **32** (1961) 308.
7. J.M. Brown, *J. Appl. Physics* **86** (1999) 5801.
8. A.P. Hammersley, *ESRF Internal Report, FIT2D V9.129* (1998).